Nano Today 50 (2023) 101889

Contents lists available at ScienceDirect

Nano Today

journal homepage: www.elsevier.com/locate/nanotoday

Functional mass nanoprobes inserted on live cells for *in situ* monitoring multiple secreted enzymes with MALDI-TOF mass spectrometry

Nan Feng, Yiran Li, Jiahui Sun, Haiqi Wang, Qiulin Ma, Jingxing Guo, Huangxian Ju *

State Key Laboratory of Analytical Chemistry for Life Science, School of Chemistry and Chemical Engineering, Nanjing University, Nanjing 210023, PR China

ARTICLE INFO

Article history:
Received 25 February 2023
Received in revised form 7 May 2023
Accepted 24 May 2023
Available online xxxx

Keywords:
Mass nanoprobe
In situ detection
MALDI-TOF MS
Dynamic quantification
Cell secretion

ABSTRACT

Numerous enzymes secreted from tumor cells have been used as biomarkers for early diagnosis, but *in situ* monitoring their secretion is still a challenge owing to the low amount and diffusion into complex environment. Herein, we establish a mass spectrometric protocol for *in situ* dynamic biosensing of multiplexed enzyme secretions by inserting tentacle-like mass nanoprobes on live cells. The nanoprobes are designed to contain an inserting group for cell anchoring and abundant substrate peptides for mass coding to facilely capture the secreted target enzymes followed with *in situ* MALDI-TOF MS detection. From the peaks of the substrates and their cleavage products, the quantification strategy of the corresponding secreted enzyme is achieved. Taking MMP-2 and MMP-9 as targets, the *in situ* monitoring protocol is demonstrated to provide a high-throughput technique for rapid detection of multiple secreted enzymes. Its universality for more secreted enzymes is also verified with cell-secreted urokinase-type plasminogen activator and alkaline phosphatase. The results identical to those from conventional phenotype methods for assessment of drugs efficacy indicate the promising application of the proposed protocol.

Introduction

The complexity and trickery of cancer present considerable hurdles to its diagnosis and therapy. Many attempts have been made from various facets to identify biomarkers for tumor screening, clinical staging, therapeutic effects evaluation and adverse events prediction [1,2]. Some cell-secreted enzymes have been considered to be significant biomarkers in clinical diagnosis of cancers [2,3]. However, their performances are less convincing due to following reasons: 1) tumor heterogeneity leads to low specificity and sensitivity, 2) it is difficult to detect low-abundance biomarkers when they diffuse into extracellular environment, 3) non-*in situ* assay results in less precision and the loss of spatiotemporal information. Thus, it is an urgent need to develop *in situ* monitoring protocols for the secretion of specific enzymes from cells.

To solve the detection sensitivity for cell-secreted enzymes, Han and coworkers took the advantages of microfluidics to concentrate matrix metalloproteinases (MMPs) from diluted cellular supernatant [4], Lou et al. confined aggregation-induced emission molecules in nanostructure to enhance the aggregation degree responding to cell-secreted MMP-2 [5], and Duffy group developed a single-molecule enzyme-linked immunosorbent assay to detect aM-level prostate-specific antigen in serum [6]. Nevertheless, these methods cannot realize the *in situ* monitoring of cell-secreted enzymes due to the need of signal amplification. Therefore, several strategies have been proposed for secretion monitoring by changing the refractive index of photonic crystal by MMPs in the entire pore spaces [7], and influencing the stacked guanine-quenched photoinduced electron transfer [8], solid-state fluorochrome precipitation [9] and peptide assembly on ionic nanochannel [10] with enzymes in extracellular matrix. A surface-enhanced Raman scattering assay has been proposed for MMP-2 analysis with the signal ratio of peptide substrate to internal standard on AuNPs [11]. A membrane-anchoring DNA nanodevice has also been designed to respond MMP-2/9 and ATP in extracellular tumor microenvironment [12]. Obviously, the cell-secreted targets diffuse into extracellular environment when they are detected, which inevitably loses some information related to the biochemical and cellular functions of enzymes. Although a phosphorylated lipid-conjugated oligonucleotide has been constructed for alkaline phosphatase (ALP)-dependent cell membrane adhesion by enzymatic dephosphorylation [13], it cannot be used for *in situ* detection of secreted enzymes. To achieve the real *in situ* dynamic

* Corresponding author.
E-mail address: hxju@nju.edu.cn (H. Ju).

https://doi.org/10.1016/j.nantod.2023.101889
1748-0132/

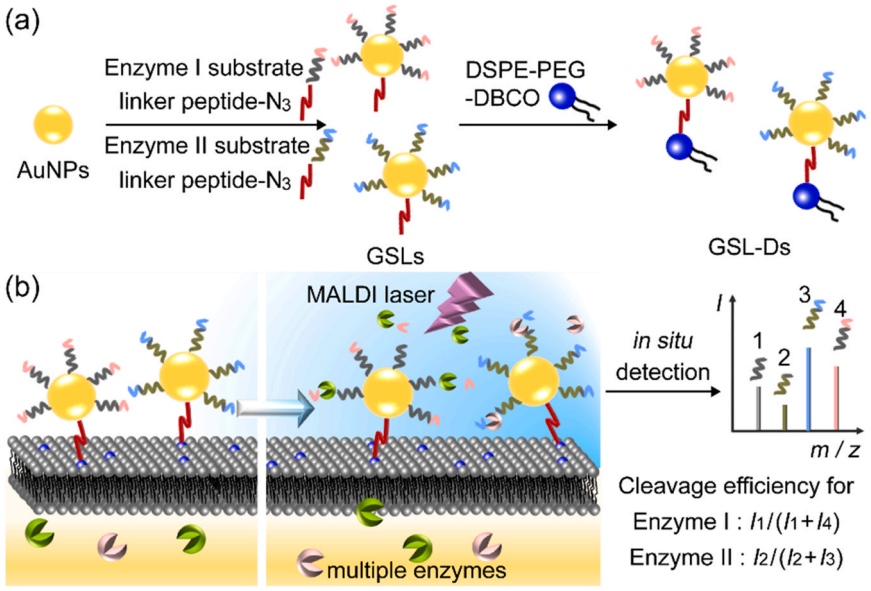

Fig. 1. Schematic illustrations of mass nanoprobe synthesis and *in situ* MALDI-TOF MS sensing of cell-secreted enzymes. (a) Synthesis of mass nanoprobes with AuNPs, substrate peptide, linker peptide-N_3 and DSPE-PEG-DBCO. (b) Scheme of *in situ* dynamic MALDI-TOF MS detection principle for multiple enzymes secreted from living cells with the mass nanoprobes.

monitoring, this work designed two functional mass nanoprobes and developed a diffusion-free strategy to rapidly respond multiple secreted enzymes by inserting the tentacle-like nanoprobes on live cells followed with matrix-assisted laser desorption/ionization-time of flight (MALDI-TOF) mass spectrometric (MS) detection.

MS techniques have extensively been used for proteomics quantification [14], biomarker detections [15–18] and drug screening [19,20] due to the unique mass resolution and the advantage of label-free analysis. Among these techniques, MALDI-TOF MS can be conveniently integrated with the molecular recognition by immobilizing the recognition element on a chip to greatly simplify the analytical procedure, and thus has been used for the profiling of enzyme activity [17,21] and biological interaction [22], the screening of drugs or inhibitors [23], the mapping of metabolites [24], and the discrimination of glycopeptides [25], *etc.* Recently, cell-based MALDI-TOF MS technology has been proposed for visualizing drug distribution in subcellular locations [26] and analyzing the extracted contents [27]. Here the designed tentacle-like mass nanoprobes contained an inserting group, thus could directly insert into the membrane of living cells that were previously seeded on an indium tin oxide (ITO) glass slide (Fig. 1). The abundant substrate peptides on the anchored nanoprobe could act as artificial tentacles to sense the enzyme secretion. Interestingly, different nanoprobes could be inserted on the same cells for diffusion-free sensing of multiple secreted enzymes. Moreover, the enzyme capture could quickly happen upon the cell secretion due to the short distance between substrate peptides and cell membrane. By changing the sequence of peptides, different mass shifts as the peptide codes could be obtained for multiple target enzymes. Through mass coding, the MALDI-TOF MS quantification of multiple secreted enzymes could be achieved from the MS peaks of the substrates and their cleavage products.

Disease-related enzymes are generally potential drug targets. Thus the activity-based profiling of enzymes has become a powerful protocol for drug efficacy assessment [28,29]. To demonstrate the practicability of the *in situ* quantitation strategy of living cell-secreted enzyme activity, the proposed method was used for *in situ* dynamic monitoring of MMP-2 and MMP-9 secreted from MDA-MB-231 and HT-1080 cells upon lipopolysaccharide (LPS) stimulation. Three inhibitors, 1,10-phenanthroline (phen), ilomastat and ARP-100, were chosen to examine its application in drug efficacy assessment by comparing the results with those from wound-scratch and transwell invasion assays [30–32]. Its universality for more secreted enzymes is also verified with cell-secreted urokinase-type plasminogen activator (uPA) and ALP. Thus, the proposed protocol possesses the promising application in biomedicine.

Methods

Synthesis of AuNPs

N-(2-Mercaptopropionyl) glycine (0.1 mmol) was dissolved in 1.75 mL 6:1 (v/v) methanol/acetic acid, and mixed with 1.4 mL 1% gold(III) chloride trihydrate. After the color of the mixture became lighter with continuous stirring, $NaBH_4$ (0.68 mmol) in 170 μL water was added, and the solution turned black suddenly. The solution was continuously stirred for 2 h to collect the product *via* concentration under vacuum to 1 mL, which was diluted with 1 mL water, and dialyzed (MWCO=5000) with Mill-Q water for more than 72 h, and the water was changed every 10–12 h [33].

Synthesis of mass nanoprobes (GSL-Ds)

200 μL of the obtained AuNPs, 16 μL 1 mM linker peptide-N_3 and 80 μL 1 mM substrate peptide for MMP-2, MMP-9, uPA or ALP were added to 704 μL 4-(2-hydroxyethyl)piperazin-1-ethanesulfonic acid (HEPES) buffer (50 mM, pH 6.5). After reaction at room temperature (RT) for 4 h, the functional AuNPs were ultrafiltrated for 10 times to remove excess peptide, and concentrated to 200 μL to obtain GSLs, which was then mixed with 800 μL 1,2-distearoyl-sn-glycero-3-phosphoethanolamine-N-[dibenzocyclooctyl (polyethylene glycol)] (DSPE-PEG-DBCO, 75 μM) in PBS for 2 h to get the mass nanoprobe GSL-Ds.

Cell culture

Human breast cancer cell lines MDA-MB-231 and MCF-7, human cervical cancer cell line HeLa, human hepatocellular carcinoma cell line HepG2 and human normal breast cell line MCF 10 A were purchased from Jiangsu KeyGEN BioTECH Co., Ltd. (Nanjing, China).

Human fibrosarcoma cell line HT-1080 was obtained from National Collection of Authenticated Cell Cultures (Shanghai, China). MDA-MB-231, HeLa and HepG2 cells were cultured in Dulbecco's modified Eagle's medium (DMEM), HT-1080 cells were cultured in minimum essential medium (MEM), MCF 10 A and MCF-7 cells were cultured in RPMI-1640. All the media contained 10% fetal bovine serum (FBS), penicillin (100 U mL^{-1}) and streptomycin (100 μg mL^{-1}), and all the cells were cultured at 37 °C under a humidified 5% CO_2 atmosphere.

Insertion of DSPE on cell membrane

4000 cells were seeded on a circular area with 4-mm diameter on ITO glass slide, and cultured for 12 h. After the cells were washed for three times with phosphate buffer saline (PBS), 10 μL mass nanoprobe GSL-D or mixture of GS^{M2}L-D and GS^{M9}L-D (1:1) was dropped on each area and left for 10 min at RT, during which the nanoprobes were inserted on cellular membrane *via* DSPE. After the cells were washed for three times with PBS to remove excess nanoprobes, they were used for the *in situ* monitoring of MMP-2, MMP-9, uPA or ALP secretion from the cells *via* the MALDI-TOF MS sensing tentacles with α-cyano-4-hydroxycinnamic acid (CHCA) as matrix.

As control, confocal laser scanning microscope (CLSM) imaging or flow cytometry assays were performed to demonstrate the insertion capability of DSPE by incubating MDA-MB-231 cells with 75 μM 1,2-distearoyl-sn-glycero-3-phosphoethanolamine-N-[(polyethylene glycol)]-fluorescein isothiocyanate (DPSE-PEG-FITC) in PBS for 10 min at RT, and followed by washing thrice with PBS [13,34].

For cytotoxicity assay of the mass nanoprobe insertion, 10,000 cells were seeded into each well on 96-well plate and cultured for 24 h. After washing twice with PBS, the cells were incubated with 25 μL mass nanoprobe for 10 min at RT. After washing the cells with PBS for three times, the cells were cultured in 10% FBS media for 2 h at 37 °C to perform cell viability assays with Cell Counting Kit-8 (CCK-8).

For localizing GSL-D on cell membrane, MDA-MB-231 and MCF-7 cells were digested with trypsin, stained with 10 μM 3,3'-dioctadecyloxacarbocyanine perchlorate (DiO) for 15 min at 37 °C, incubated with GS^{M2}L-D for 10 min at RT, and then stained with 15 μg mL^{-1} streptavidin (SA)-Cy5 for 30 min at 4 °C. These cells were finally seeded on confocal dish to perform CLSM imaging immediately.

Calibration curves for detection of enzymes concentrations

To obtain the calibration curves of each enzyme, MMP-2 and MMP-9 (1 μg mL^{-1}) were firstly activated with 1 mM 4-aminophenylmercuric acetate (APMA) in reaction buffer (50 mM Tris(hydroxymethyl)aminomethane (Tris), 10 mM $CaCl_2$, 150 mM NaCl pH 7.5) at 37 ℃ for 1 h, and then diluted to the known concentrations with the buffer. And uPA was directly diluted with HEPES buffer (20 mM HEPES, 2 mM $CaCl_2$ pH 7.4), and ALP was diluted with Tris-HCl buffer (10 mM Tris, 2 mM $MgCl_2$, 0.1 mM $ZnCl_2$ pH 8.0). Meanwhile, 4000 MDA-MB-231 cells seeded on ITO glass slide were fixed with 4% paraformaldehyde for 15 min at RT, and incubated with 10 μL mass nanoprobe GSL-D or mixture of GS^{M2}L-D and GS^{M9}L-D (1:1) for 10 min at RT. After the cells were washed with PBS for three times, 10 μL standard solution of corresponding enzyme was dropped on the cells area to react at 37 ℃ for 30 min. Afterward, MALDI-TOF MS analysis was carried out with 2 μL CHCA in the mixture of acetonitrile, water and trifluoroacetic acid (50:49.9:0.1, v/v/v) as matrix.

In situ monitoring of secreted enzymes

In order to stimulate the secretion of MMPs from living cells, the cells were treated with starvation or LPS. Starvation treatment was performed by culturing MDA-MB-231 cells seeded on an ITO glass slide in serum-free media for 12 h, washing them with PBS, and then incubating them with 10 μL mass nanoprobe GS^{M2}L-D, GS^{M9}L-D or their mixture (1:1) for 10 min at RT. These cells were then washed for three times with PBS, and cultured in 10 μL serum-free media at 37 ℃ for different times to *in situ* detect the secreted MMPs with 2 μL 10 mg mL^{-1} CHCA in the mixture of acetonitrile, water and trifluoroacetic acid (50:49.9:0.1, v/v/v) as matrix.

LPS-treated cells were prepared by incubating Hela, MCF 10 A, MCF-7, MDA-MB-231 or HT-1080 cells seeded respectively on ITO glass slides in 10 μL mass nanoprobe for 10 min at RT, washing them with PBS, and then cultured them in serum-free media containing 50 μg mL^{-1} LPS at 37 ℃ to *in situ* detect the secreted MMPs at different times. The inhibition of different drugs to the secreted MMPs was monitored by adding 250 μM phen [35], 10 μM ilomastat [36,37] or 50 nM ARP-100 [38] in serum-free media containing 50 μg mL^{-1} LPS to incubate for 2 h. For obtaining the inhibition curves of MMPs with inhibitors phen or ilomastat, HT-1080 cells on ITO glass slide were incubated with 10 μL mass nanoprobe GS^{M2}L-D or GS^{M9}L-D for 10 min at RT, and then cultured in serum-free media containing 50 μg mL^{-1} LPS by adding phen (1–1000 μM) or ilomastat (1–500 μM) to incubate for 2 h.

For monitoring secreted uPA from living cells, MCF-7, MDA-MB-231 or HT-1080 cells were seeded respectively on ITO glass slides, incubated with 10 μL mass nanoprobe GS^{uPA}L-D for 10 min at RT, washed with PBS, and then cultured in serum-free media for 2 h. For inhibition study, MDA-MB-231 or HT-1080 cells were pretreated with 50 μM 4-chlorophenylguanidine hydrochloride (4-CPG) for 1 h [39], incubated with 10 μL mass nanoprobe GS^{uPA}L-D for 10 min at RT, and then cultured in serum-free media containing 50 μM 4-CPG for 2 h.

For monitoring ALP, HepG2 cells on ITO glass side were incubated with 10 μL mass nanoprobe GS^{ALP}L-D for 10 min at RT, washed with PBS, and then cultured in serum-free media for 2 h. For inhibition study, HepG2 cells were pretreated with 100 μM Na_3VO_4 for 30 min [13], incubated with 10 μL mass nanoprobe GS^{uPA}L-D for 10 min at RT, and then cultured in serum-free media containing 100 μM Na_3VO_4 for 2 h.

For examining the residence time of mass nanoprobe on cell membrane, MCF-7 cells were treated with GS^{M2}L-D for 10 min, washed with PBS, incubated in culture medium for 1, 2, 4 h at 37 °C, and then stained with 15 μg mL^{-1} SA-Cy5 for 30 min at 4 °C to perform CLSM imaging immediately.

Wound-scratch assays of cell migration

After MCF-7, MDA-MB-231 or HT-1080 cells were seeded in 24-well plates and cultured overnight, a 10 μL pipette tip was used to scratch a wound through the center of each well. After washing with PBS for three times, the cells were treated with serum-free media containing an inhibitor (250 μM phen, 10 μM ilomastat or 50 nM ARP-100) and 50 μg mL^{-1} LPS at 37 ℃. As control, the cells were cultured in serum-free media containing 50 μg mL^{-1} LPS. Cell images were captured immediately and after 24-h incubation. Data analysis was performed using Image J software.

Tanswell invasion assays

100 μL 0.2 mg mL^{-1} matrigel was added in 24-well transwell inserts (Corning) and left overnight at 37 ℃. After adding 200 μL serum-free media containing 50 μg mL^{-1} LPS, 0.2% bovine serum albumin (BSA) and 50,000 cancer cells in absence as control and presence of an inhibitor (250 μM phen, 10 μM ilomastat or 50 nM ARP-100) to upper chamber and 700 μL 20% FBS media to lower chamber, the transwell invasion assay was performed after 24-h incubation at 37 ℃. Afterward, the upper chambers were taken out and washed twice with PBS, and the invading cells were fixed with iced methanol for 30 min at 4 ℃, stained with 0.1% crystal violet staining solution for 20 min at RT to capture the cells images immediately.

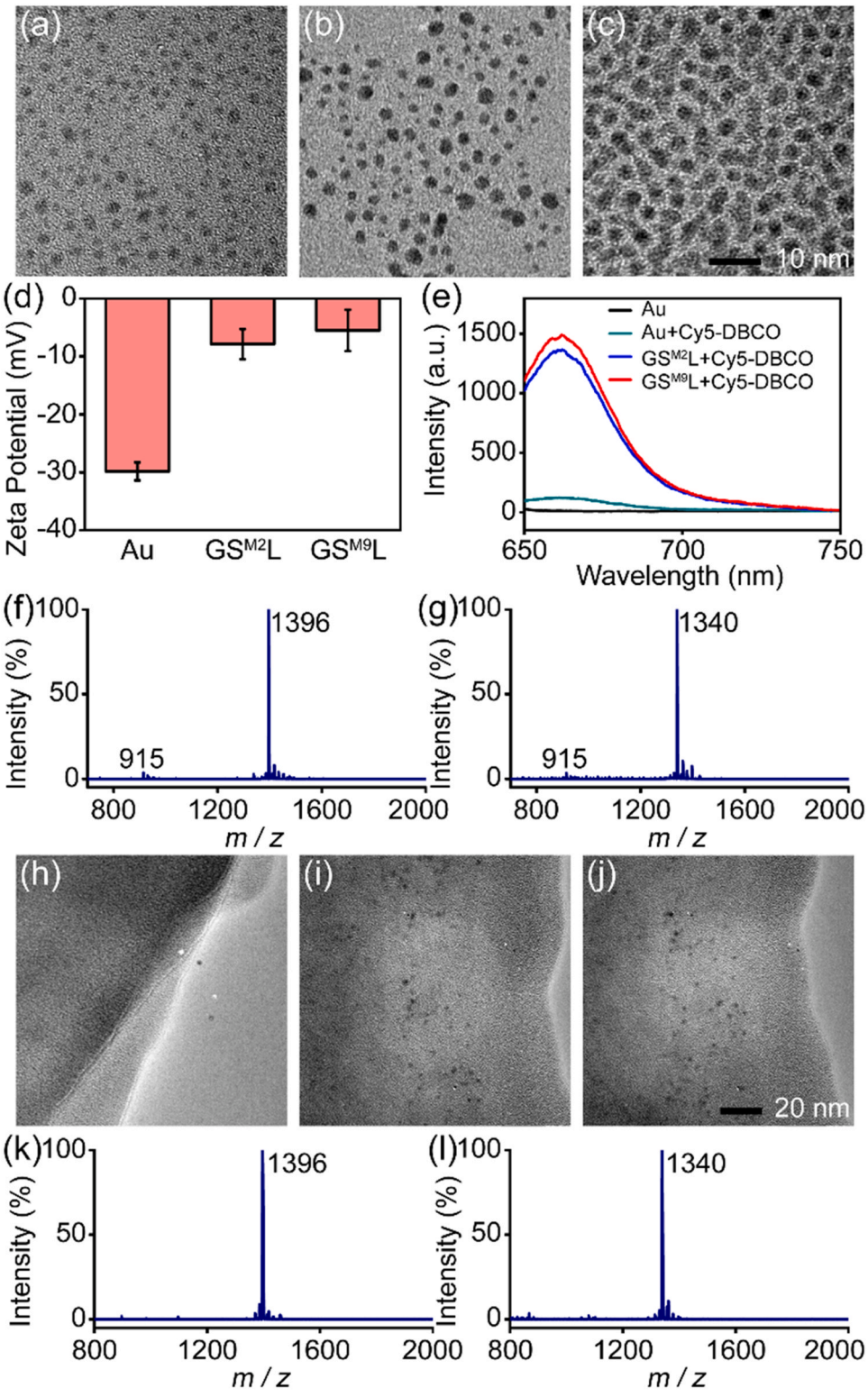

Fig. 2. Characterizations of AuNPs, GSLs and mass nanoprobes (GSL-Ds). (a-c) TEM images and (d) Zeta potentials of AuNPs (a), $GS^{M2}L$ (b) and $GS^{M2}L$-D (c). (e) Fluorescence spectra of AuNPs and the mixtures of Cy5-DBCO with AuNPs, $GS^{M2}L$ or $GS^{M9}L$ after incubation for 2 h. (f, g) Mass spectra of $GS^{M2}L$ (f) and $GS^{M9}L$ (g). (h-j) TEM images of MDA-MB-231 cells incubated with $GS^{M2}L$, $GS^{M2}L$-D and $GS^{M9}L$-D for 10 min at RT. (k, l) Mass spectra of seeded MDA-MB-231 cells after incubation with $GS^{M2}L$-D (k) and $GS^{M9}L$-D (l).

Results and discussion

Characterization of mass nanoprobes

To fabricate the mass nanoprobes for MMP-2 and MMP-9, AuNPs were first synthesized by reducing $HAuCl_4$ with $NaBH_4$ [33], which showed a homogeneous size of 2 nm (Fig. 2a). After the substrate peptide for MMP-2 (sub-2) or MMP-9 (sub-9) and linker peptide-N_3 were loaded on AuNPs through Au-NH_2 or Au-S bond, the obtained $GS^{M2}L$ or $GS^{M9}L$ was purified *via* ultrafiltration with water for 10 times (Fig. S1), and showed the same size as AuNPs (Fig. 2b). Although the peptide loading decreased the Zeta potential (Fig. 2d),

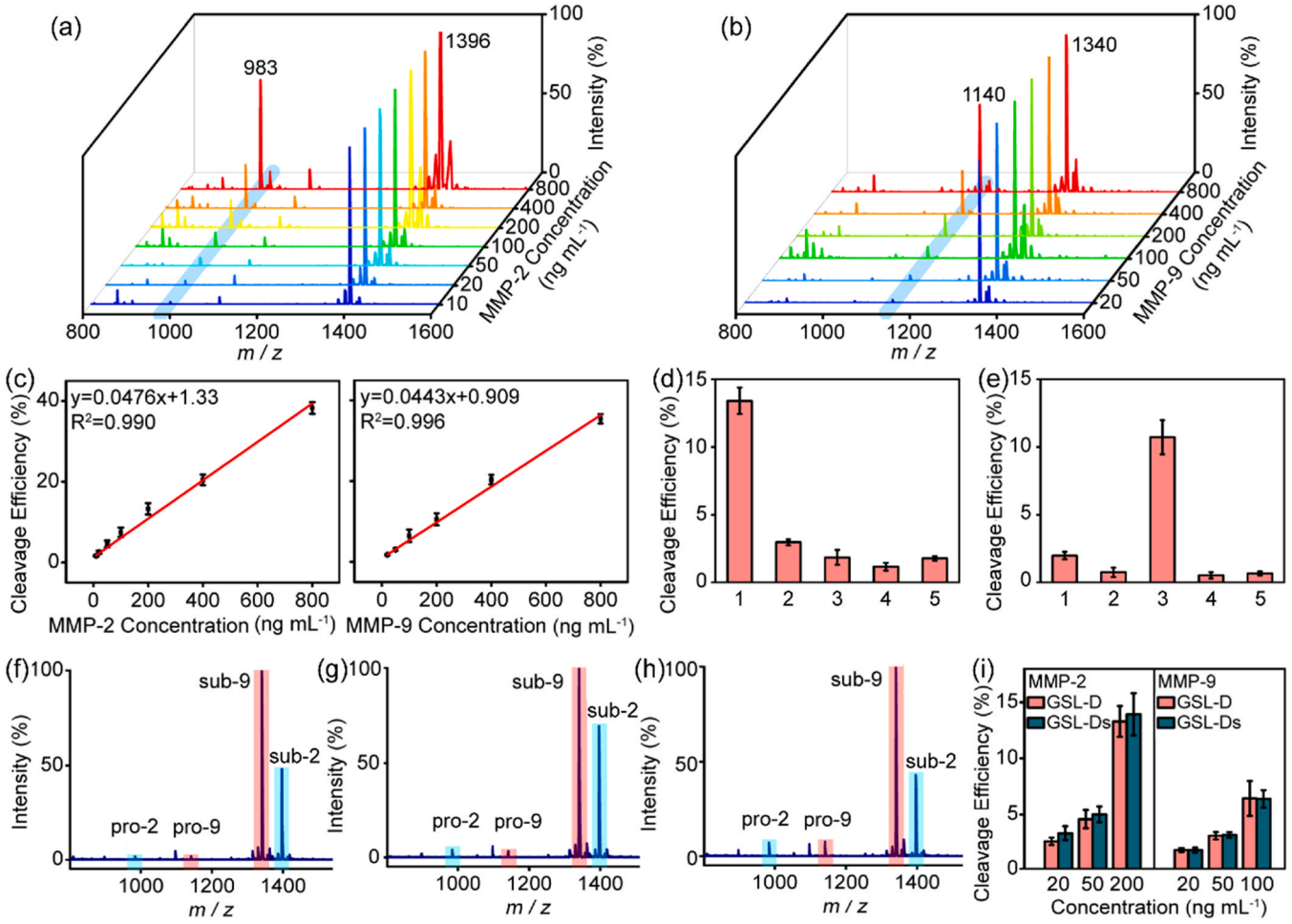

Fig. 3. Feasibility of *in situ* MS quantification of secreted MMPs. (a, b) Mass spectra of 4% paraformaldehyde fixed MDA-MB-231 cells after inserting $GS^{M2}L$-D (a) or $GS^{M9}L$-D (b) and then incubating with10–800 ng mL^{-1} MMP-2 (a) or 20–800 ng mL^{-1} MMP-9 (b) for 30 min. (c) Calibration curves of cleavage efficiency at 30 min *vs* MMP-2 and MMP-9 concentration. (d, e) Selectivity test of $GS^{M2}L$-D and $GS^{M9}L$-D inserted MDA-MB-231 cells for incubation with 200 ng mL^{-1} MMP-2 (1), 200 ng mL^{-1} MMP-2 (d) or MMP-9 (e) in presence of 250 μM inhibitor phen (2), 200 ng mL^{-1} MMP-9 (3), 200 ng mL^{-1} BSA (4), 30 U mL^{-1} Neu (5) for 30 min. (f-h) Mass spectra of 4% paraformaldehyde fixed MDA-MB-231 cells after inserting $GS^{M2}L$-D and $GS^{M9}L$-D and then incubating with 20 (f) and 50 (g) ng mL^{-1} MMP-2 and MMP-9, and 200 ng mL^{-1} MMP-2 and 100 ng mL^{-1} MMP-9 (h) for 30 min. (i) Cleavage efficiency for MMP-2 and MMP-9 obtained from (a, b and f-h).

the negatively charged surface endowed the product with similar dispersity to AuNPs. The presence of free azido group was demonstrated with the fluorescence spectra of the reaction product of GSLs with Cy5-DBCO, which showed the fluorescence of Cy5 (Fig. 2e). The mass spectra of $GS^{M2}L$ and $GS^{M9}L$ showed the characteristic peaks of linker peptide-N_3 at *m*/*z* of 915 ($[M+Na]^+$), sub-2 at *m*/*z* of 1396 ($[M+H]^+$) and sub-9 at *m*/*z* of 1340 ($[M+H]^+$) (Fig. 2f, g). The free azido groups on $GS^{M2}L$ and $GS^{M9}L$ were finally conjugated with DSPE-PEG-DBCO to obtain the mass nanoprobes $GS^{M2}L$-D and $GS^{M9}L$-D, which indicated larger size than GSLs (Fig. 2c). From the UV-Vis absorption spectrum of $GS^{M2}L$-D, its concentration was calculated to be 2.38 μM according to Lambert-Beer law and the molar extinction coefficient of AuNPs at 450 nm (Fig. S2) [40].

Owing to the similar phospholipid structure of DSPE with cells membrane [41], the DSPE conjugated on the mass nanoprobes could insert into cell membrane through a simply incubation step [34,42,43]. The incubation time was optimized with flow cytometry to be 10 min by mixing DSPE-PEG-FITC and MDA-MB-231 cells for different times (Fig. S3a), at which the confocal images showed the fluorescence of FITC on cell surface (Fig. S3b). Compared to $GS^{M2}L$-D and $GS^{M9}L$-D, $GS^{M2}L$ could not insert into the cell membrane due to the absence of DSPE (Fig. 2h-j). After treating MDA-MB-231 or MCF-7 cells with membrane dye DiO, $GS^{M2}L$-D and then SA-Cy5, which could localize mass nanoprobe *via* the interaction of SA with biotin on peptide substrate (Table S1), the Cy5 fluorescence mainly occurred on the outer side of cell membrane (Fig. S4), and could maintain for 4 h (Fig. S5), indicating that the mass nanoprobe could stay on the membrane stably. Moreover, the mass spectra of $GS^{M2}L$-D or $GS^{M9}L$-D treated cells (Fig. S6) revealed the signals of the mass nanoprobes at *m*/*z* 1396 and 1340, respectively (Fig. 2k, l), confirming their successful cell anchoring.

Feasibility of in situ MS quantification of secreted MMPs

To perform *in situ* MS biosensing of multiple cell-secreted MMPs, the synthesis conditions of the mass nanoprobes were optimized with standard enzyme solution after anchoring the obtained nanoprobes on 4% paraformaldehyde fixed MDA-MB-231 cells. Here, the fixing treatment was used to terminate the enzyme secretions. The MALDI-TOF mass spectra of the enzyme incubated cells anchoring the mass nanoprobes showed the peaks of sub-2 and sub-9 at *m*/*z* 1396 and 1340, and the peaks of their enzymatic hydrolysis products (pro-2 and pro-9) at *m*/*z* 983 and 1140, respectively (Fig. 3a, b). Therefore, the enzymatic cleavage efficiency could be obtained from the peak intensities with $I_{product}/(I_{substrate}+I_{product})^* 100\%$ (Fig. 1) [21,44]. The maximum cleavage efficiency occurred at the substrate-to-linker peptide ratio of 5:1 (Fig. S7), at which the optimal reaction time was 30 min (Fig. S8). The calibration curves for detecting the

concentrations of cell-secreted MMP-2 and MMP-9 could thus be obtained with their standard solutions and the nanoprobes anchored MDA-MB-231 cells (Fig. 3a-c). The cleavage efficiencies were proportional to MMP-2 and MMP-9 concentrations in 10–800 and 20–800 ng mL^{-1}, which resulted in the limits of detection of 5.78 and 8.80 ng mL^{-1} at 3σ, respectively. The specificity of the designed mass nanoprobes to MMPs was further examined by incubating GS^{M2}L-D or GS^{M9}L-D inserted MDA-MB-231 cells after fixed in reaction buffer containing MMP-2, MMP-9, MMP with inhibitor phen, BSA or neuraminidase (Neu). Except the corresponding MMPs, all other proteins showed negligible cleavage efficiency (Fig. 3d, e), suggesting the good specificity of both mass nanoprobes. The detection accuracy for MMPs was also demonstrated by the identical results obtained from the proposed method and human MMP-2 ELISA kit (Fig. S9). Thus, the feasibility using the proposed method to *in situ* quantify cell-secreted MMP-2 or MMP-9 was verified.

The simultaneous quantification of multiple enzymes secreted from the same cells was demonstrated by anchoring two GSL-D nanoprobes on the fixed cells to measure the MALDI-TOF mass spectra after incubating them with MMPs (Fig. 3f-h). At different MMPs concentrations, the obtained results were identical to those from single mass nanoprobe anchored cells (Fig. 3i), indicating the feasibility using the proposed method to sense multiple enzyme secretions.

In situ sensing of cell secreted enzymes from various cell lines

To achieve the practical application of the designed mass nanoprobes in *in situ* dynamically monitoring enzyme secretions of living cells, their cell cytotoxicity was tested with CCK-8, which demonstrated negligible influence on different cell lines (Fig. S10). Thus different mass nanoprobes could be anchored on living cells to monitor the MMP secretions. Using MDA-MB-231 cells, which highly express MMPs [45] and can secrete MMP-2 and MMP-9 upon starvation or LPS stimulation [46] as model, the mass spectra showed the increasing signal ratios of pro-2 to sub-2 and pro-9 to sub-9 with the increasing stimulation time (Fig. 4a, b), which indicated the

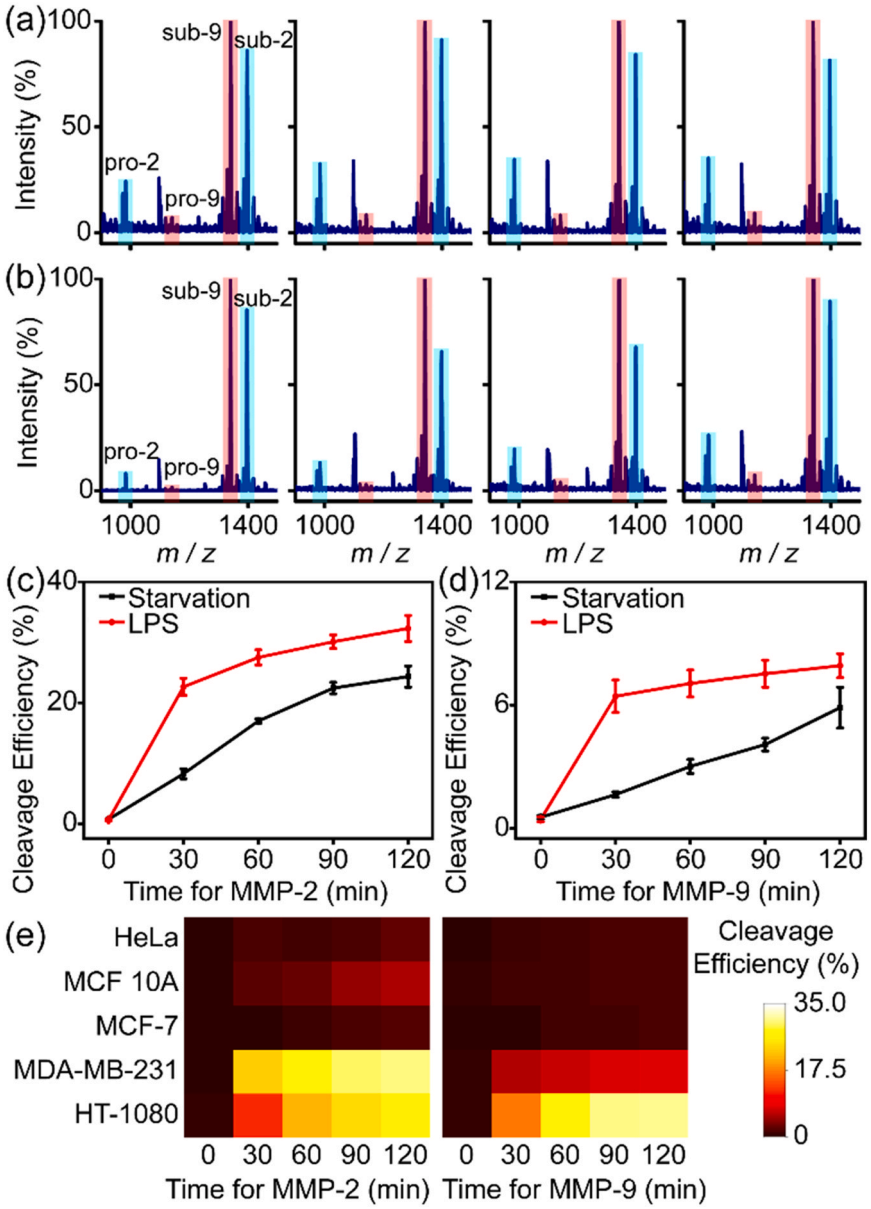

Fig. 4. *In situ* sensing of cell secreted enzymes from various cell lines. (a, b) Mass spectra of GS^{M2}L-D and GS^{M9}L-D inserted MDA-MB-231 cells after treatment with 50 μg mL^{-1} LPS (a) or starvation (b) for 30, 60, 90 and 120 min (from left to right). (c, d) Plots of cleavage efficiency from (a, b) *vs* treatment time. (e) Heatmaps of cleavage efficiency of MMP-2 and MMP-9 secreted from Hela, MCF 10 A, MCF-7, MDA-MB-231 and HT-1080 cells after treated with 50 μg mL^{-1} LPS for different times.

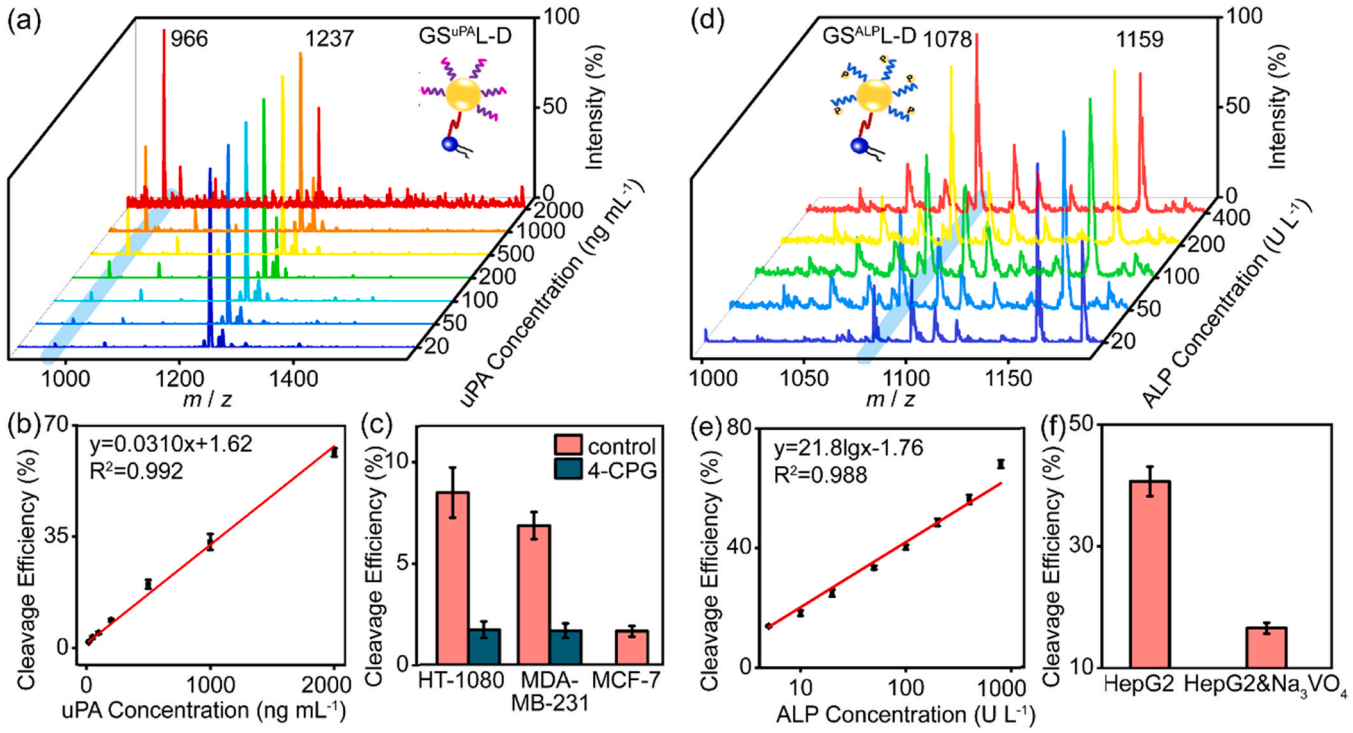

Fig. 5. Universality of the proposed method. (a, d) Mass spectra of 4% paraformaldehyde fixed MDA-MB-231 cells after inserting GS^{uPA}L-D (a) or GS^{ALP}L-D (d) and then incubating with 20–2000 ng mL^{-1} uPA or 20–400 U L^{-1} ALP for 30 min (b, e) Corresponding calibration curves. (c) Cleavage efficiency of uPA secreted from HT-1080, MDA-MB-231 or MCF-7 cells after treatment with 50 μM 4-CPG for 2 h. (f) Cleavage efficiency of ALP secreted from HepG2 cells after treatment with 100 μM Na_3VO_4 for 2 h.

increasing enzymatic cleavage efficiency (Fig. 4c, d). From the cleavage efficiency and the calibration curves shown in Fig. 3c, the concentrations of MMP-2 and MMP-9 secreted from starvation and LPS treated MDA-MB-231 cells could be obtained. The 2-h stimulation resulted in the MMP-2 and MMP-9 concentrations around cell membrane to be 483 and 112 ng mL^{-1} for starvation, and 650 and 158 ng mL^{-1} for LPS, respectively. These results were the same as those detected with single mass nanoprobe anchored MDA-MB-231 cells (Figs. S11 and S12), demonstrating a rapid and high-throughput method for *in situ* dynamic quantification of multiplexed enzyme secretions from living cells.

To verify the practical application, the mass nanoprobes were anchored onto more cell lines to sense MMP secretions from MCF-7, MCF 10 A and HeLa cells, scarcely expressing MMP-2 and MMP-9, and HT-1080 cells with high expressions of these MMPs [46,47]. Upon LPS stimulation, HT-1080 cells showed the increase of enzymatic cleavage efficiency of both MMP-2 and MMP-9 to the maximum value (Figs. S13 and Fig. 4e). The latter was even higher than that from MDA-MB-231 cells. Predictably, MCF 10 A cells only showed slight increase of MMP-2, and other cells did not show the presence of both MMP-2 and MMP-9 (Fig. 4e), consistent with previous reports [46,47].

Universality of the proposed method

The proposed method was also used for *in situ* monitoring the secretion of uPA and ALP from live cells. The corresponding mass nanoprobe GS^{uPA}L-D or GS^{ALP}L-D and their insertion on MDA-MB-231 cells were demonstrated with Zeta potentials, fluorescence spectra, TEM images and mass spectra (Fig. S14). The mass spectrum of mass nanoprobe GS^{uPA}L-D or GS^{ALP}L-D anchored MDA-MB-231 cells showed the peaks of substrate and its hydrolysis product for uPA at *m*/*z* 1237 and 966 or ALP at 1159 and 1078, respectively (Fig. 5a, d). According to the calibration curves (Fig. 5b, e), the enzymatic cleavage efficiency was proportional to the concentrations of uPA in 20–2000 ng mL^{-1} and ALP in 5–800 U L^{-1} with the limits of detection of 6.90 ng mL^{-1} and 4.96 U L^{-1}, respectively.

The *in situ* monitoring results indicated that HT-1080 and MDA-MB-231 cells possessed strong uPA secretion, which was attenuated obviously upon the treatment of inhibitor 4-CPG [39], while MCF-7 cells scarcely secreted uPA (Fig. 5c). Similarly, HepG2 cells showed strong ALP secretion, as previous report [13], and Na_3VO_4 could inhibited effectively the activity of secreted ALP (Fig. 5f) [13].

Drug efficacy assessment with in situ MALDI-TOF MS monitoring protocol

MMPs are closely related to physiological and pathological processes, especially cancer progression [48]. In tumor metastasis, MMP-2 can trigger cell motility [49,50] and MMP-9 can promote tumor invasion [51]. Therefore, MMP-2 and MMP-9 were taken as examples to explore the possibility of inhibitor efficacy assessment with the designed *in situ* MALDI-TOF MS monitoring protocol and conventional phenotype methods including wound-scratch and transwell invasion assays as control. In this study, three kinds of MMP inhibitors, phen, ilomastat and ARP-100, were chosen to examine the possibility. In the presence of phen, both pro-2 and pro-9 peaks from LPS stimulated MDA-MB-231 and HT-1080 cells greatly decreased, indicating good inhibition of phen to MMP-2 and MMP-9 (Fig. 6a, b), which was coincident with the previous report [52], and also demonstrated by the phenotype assays. The latter showed less migration and invasion of MDA-MB-231 and HT-1080 cells (Fig. 6c, d). Although ilomastat was also reported to be an inhibitor to MMPs from the *in vitro* assay [36], the changes of both pro-2 and pro-9 peaks from LPS stimulated MDA-MB-231 and HT-1080 cells were relatively low upon its addition (Fig. S15), showing that ilomastat could not effectively inhibit MMPs on cells, which was also demonstrated by phenotype assays. In the presence of ilomastat the migration and invasion capability of both cells only changed a little (Figs. S16-S18). ARP-100 can selectively inhibit MMP-2 and displays less inhibitory activity to MMP-9 [40]. Thus the pro-2 peaks from LPS

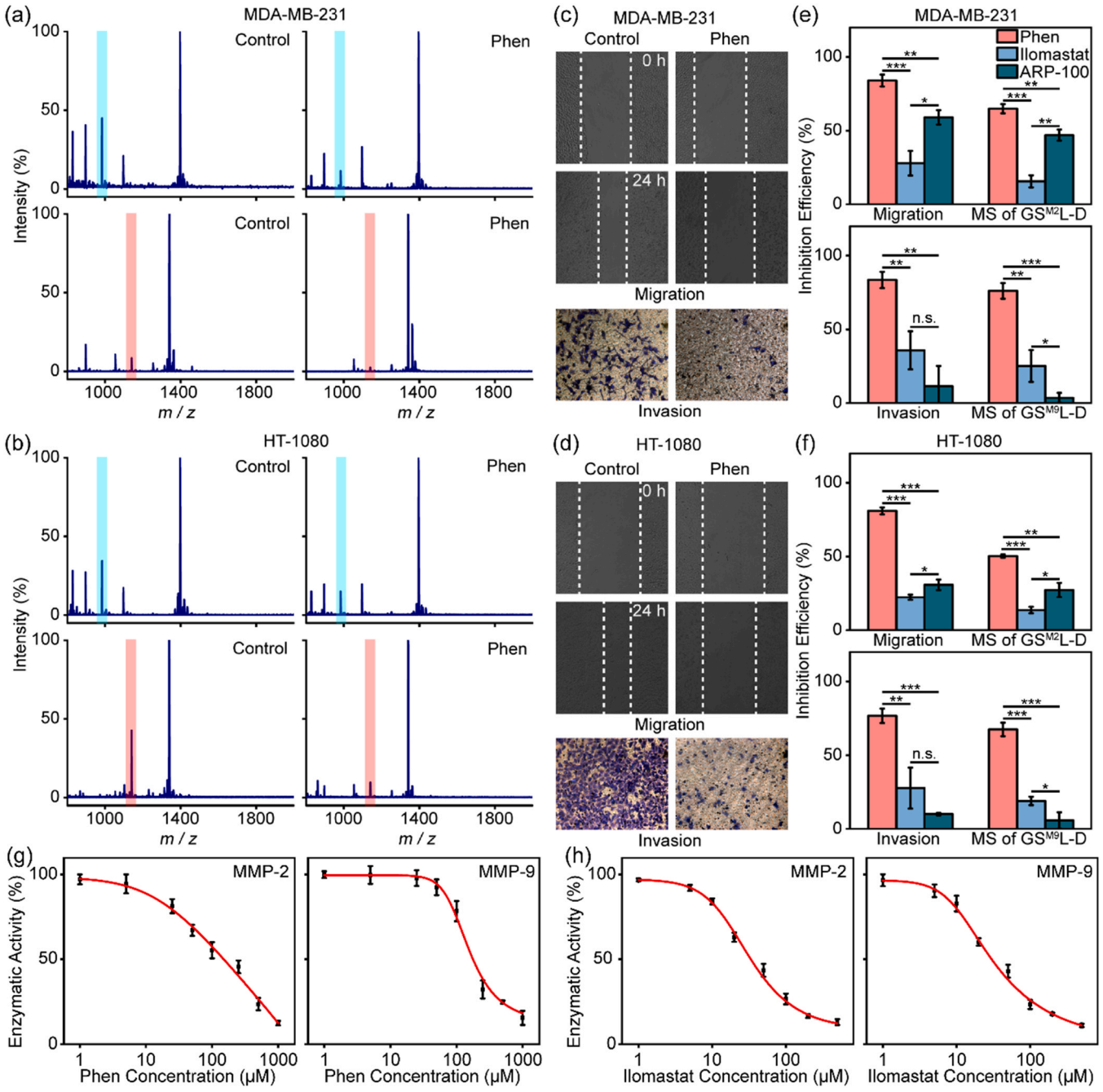

Fig. 6. Drug efficacy assessment through *in situ* MALDI-TOF MS monitoring and phenotype assays. (a, b) Mass spectra of $GS^{M2}L$-D (upper row) or $GS^{M9}L$-D (lower row) inserted MDA-MB-231 (a) and HT-1080 cells (b) after treated with serum-free media containing 50 μg mL^{-1} LPS in absence as control and presence of 250 μM phen for 2 h. (c, d) Wound-scratch and transwell invasion assay images of MDA-MB-231 and HT-1080 cells after treated with serum-free media containing 50 μg mL^{-1} LPS in absence as control and presence of 250 μM phen for 24 h. (e, f) Inhibition efficiency of 250 μM phen, 10 μM ilomastat or 50 nM ARP-100 for MDA-MB-231 (e) and HT-1080 cells (f) measured with wound-scratch, transwell invasion and mass spectrometric assays in (a)-(d), Figs. S15a and S16. (g, h) Inhibition curves of inhibitor phen (g) or ilomastat (h) on MMP-2 or MMP-9. Student's *t*-test: $^{*}p < 0.05$; $^{**}p < 0.005$; $^{***}p < 0.0005$; n.s., not significant.

stimulated MDA-MB-231 and HT-1080 cells in the presence of ARP-100 decreased, while pro-9 peak was almost unchanged (Fig. 6a, b and Fig. S15), which was coincident with the inhibited migration and unchanged invasion of both cells (Fig. 6c, d and Figs. S16-S18). The inhibition efficiencies of three inhibitors from MS detection of MMPs displayed the same ranking as those from phenotype assays (Fig. 6e, f). As a negative control, LPS stimulated MCF-7 cells displayed negligible migration and invasion (Fig. S16), which closely matched MMP-2 and MMP-9 secretions (Fig. 4e). Besides, IC_{50} of phen for MMP-2 and MMP-9 secreted from HT-1080 cells was detected to be 149 and 176 μM, respectively (Figs. 6g and S19), which was comparable to the value of 10.5 μM for MMP-2 and 16.9 μM for MMP-9 [53]. IC_{50} of ilomastat for MMP-2 and MMP-9 secreted from HT-1080 cells was 33.3 and 29.8 μM, respectively (Figs. 6h and S20). Therefore, the quantification of MMPs secreted from living cells by MALDI-TOF MS could build a bridge with drug inhibition to enzyme activity in complex environment, which provided a facile, rapid and high-throughput *in situ* MS method to evaluate the effects of drugs on enzyme biomarkers at cellular level and was expected to be commercialized for drug efficacy assessment.

Conclusion

The tentacle-like mass coding nanoprobes have been constructed for real *in situ* dynamic quantification of multiple enzymes secreted from living cells *via* anchoring the nanoprobes on cells and MALDI-TOF MS detection. This novel protocol can be achieved by the correlation of enzymatic cleavage efficiency to enzyme concentration, and the former can be obtained from the MS signals of the substrate and its hydrolysis product on the nanoprobe anchored on cells. By using different cancer cell lines as cell models and MMP-2 and MMP-9 as enzyme targets, the proposed diffusion-free sensing protocol has demonstrated its application in rapid and high-throughput drug efficacy assessment along with the coincident results with those from phenotype assays. The real *in situ* sensing method for monitoring cell secretions can distinguish the diversity of drug effects on cell secretory enzymes, and can also be expended for quantitatively monitoring the influence of exogenous molecules on cell secretion and for studying multiple biological processes including glycosylation, acetylation, and phosphorylation, *etc.* Thus, it is expected to supply *in situ* information to various fields of clinical diagnosis and drug discovery.

CRediT authorship contribution statement

Huangxian Ju: Supervised this project. **Nan Feng, Jiahui Sun**: Performed the experiments. **Nan Feng, Yiran Li, Qulin Ma, Jingxing Guo**: Analyzed the data. **Nan Feng, Yiran Li, Haiqi Wang, Huangxian Ju**: Co-wrote the manuscript. All authors discussed the results and commented on the manuscript.

Data availability

Data will be made available on request.

Declaration of Competing Interest

The authors declare that there is no conflict of interest.

Acknowledgements

This work was supported by the National Natural Science Foundation of China (21827812, 21890741) and State Key Laboratory of Analytical Chemistry for Life Science (SKLACLS2104).

Appendix A. Supporting information

Supplementary data associated with this article can be found in the online version at doi:10.1016/j.nantod.2023.101889.

References

[1] S.L. Topalian, J.M. Taube, R.A. Anders, D.M. Pardoll, Nat. Rev. Cancer 16 (2016) 275–287, https://doi.org/10.1038/nrc.2016.36
[2] V. Kulasingam, E.P. Diamandis, Nat. Clin. Pract. Oncol. 5 (2008) 588–599, https://doi.org/10.1038/ncponc1187
[3] M. Dhar, J.N. Lam, T. Walser, S.M. Dubinett, M.B. Rettig, D.D. Carlo, Proc. Natl. Acad. Sci. U. S. A. 115 (2018) 9986–9991, https://doi.org/10.1073/pnas.1803884115
[4] C.-H. Chen, A. Sarkar, Y.-A. Song, M.A. Miller, S.J. Kim, L.G. Griffith, D.A. Lauffenburger, J. Han, J. Am. Chem. Soc. 133 (2011) 10368–10371, https://doi.org/10.1021/ja2036628
[5] F. Wu, Y. Huang, X. Yang, J.-J. Hu, X.D. Lou, F. Xia, Y.L. Song, L. Jiang, Anal. Chem. 93 (2021) 16257–16263, https://doi.org/10.1021/acs.analchem.1c04422
[6] D.M. Rissin, C.W. Kan, T.G. Campbell, S.C. Howes, D.R. Fournier, L.N. Song, T. Piech, P.P. Patel, L. Chang, A.J. Rivnak, E.P. Ferrell, J.D. Randall, G.K. Provuncher, D.R. Walt, D.C. Duffy, Nat. Biotechnol. 28 (2010) 595–599, https://doi.org/10.1038/nbt.1641
[7] K.A. Kilian, L.M.H. Lai, A. Magenau, S. Cartland, T. Böcking, N.D. Girolamo, M. Gal, K. Gaus, J.J. Gooding, Nano Lett. 9 (2009) 2021–2025, https://doi.org/10.1021/nl900283j
[8] X. Su, X.C. Zhu, C. Zhang, X.J. Xiao, M.P. Zhao, Anal. Chem. 84 (2012) 5059–5065, https://doi.org/10.1021/ac300745f
[9] H.-W. Liu, K. Li, X.-X. Hu, L.M. Zhu, Q.M. Rong, Y.C. Liu, X.-B. Zhang, J. Hasserodt, F.-L. Qu, W.H. Tan, Angew. Chem. Int. Ed. 56 (2017) 11788–11792, https://doi.org/10.1002/anie.201705747
[10] L. Wang, H. Li, L. Shi, L. Li, F.J. Jia, T. Gao, G.X. Li, Biosens. Bioelectron. 195 (2022) 113671, , https://doi.org/10.1016/j.bios.2021.113671
[11] Q.M. Zhong, K. Zhang, X.D. Huang, Y.W. Lu, J.Z. Zhao, Y. He, B.H. Liu, Biosens. Bioelectron. 207 (2022) 114194, , https://doi.org/10.1016/j.bios.2022.114194
[12] Z.C. Xiang, J. Zhao, J.L. Qu, J. Song, L.L. Li, Angew. Chem. Int. Ed. 61 (2022) e202111836, , https://doi.org/10.1002/anie.202111836
[13] C. Jin, J.X. He, J.M. Zou, W.J. Xuan, T. Fu, R.W. Wang, W.H. Tan, Nat. Commun. 10 (2019) 2704, https://doi.org/10.1038/s41467-019-10639-6
[14] J. Krijgsveld, R.F. Ketting, T. Mahmoudi, J. Johansen, M. Artal-Sanz, C.P. Verrijzer, R.H.A. Plasterk, A.J.R. Heck, Nat. Biotechnol. 21 (2003) 927–931, https://doi.org/10.1038/nbt848
[15] S.M. Chen, Q.Q. Wan, A.K. Badu-Tawiah, J. Am. Chem. Soc. 138 (2016) 6356–6359, https://doi.org/10.1021/jacs.6b02232
[16] S.T. Xu, W. Ma, Y. Bai, H.W. Liu, J. Am. Chem. Soc. 141 (2019) 72–75, https://doi.org/10.1021/jacs.8b10853
[17] J.J. Hu, F. Liu, H.X. Ju, Angew. Chem. Int. Ed. 55 (2016) 6667–6670, https://doi.org/10.1002/anie.201601096
[18] Y.N. Wang, K. Zhang, X.D. Huang, L. Qiao, B.H. Liu, Anal. Chem. 93 (2021) 709–714, https://doi.org/10.1021/acs.analchem.0c03904
[19] M.S. Unger, M. Blank, T. Enzlein, C. Hopf, Nat. Protoc. 16 (2021) 5533–5558, https://doi.org/10.1038/s41596-021-00624-z
[20] M.S. Ritorto, R. Ewan, A.B. Perez-Oliva, A. Knebel, S.J. Buhrlage, M. Wightman, S.M. Kelly, N.T. Wood, S. Virdee, N.S. Gray, N.A. Morrice, D.R. Alessi, M. Trost, Nat. Commun. 5 (2014) 4763, https://doi.org/10.1038/ncomms5763
[21] N. Feng, J.J. Hu, Q.L. Ma, H.X. Ju, Biosens. Bioelectron. 157 (2020) 112159, , https://doi.org/10.1016/j.bios.2020.112159
[22] P.T. O'Kane, Q.M. Dudley, A.K. McMillan, M.C. Jewett, M. Mrksich, eaaw9180, Sci. Adv. 5 (2019), https://doi.org/10.1126/sciadv.aaw9180
[23] D.-H. Min, W.-J. Tang, M. Mrksich, Nat. Biotechnol. 22 (2004) 717–723, https://doi.org/10.1038/nbt973
[24] H.-Y. Kuo, T.A. DeLuca, W.M. Miller, M. Mrksich, Anal. Chem. 85 (2013) 10635–10642, https://doi.org/10.1021/ac402614x
[25] P. Both, A.P. Green, C.J. Gray, R. Sardzik, J. Voglmeir, C. Fontana, M. Austeri, M. Rejzek, D. Richardson, R.A. Field, G. Widmalm, S.L. Flitsch, C.E. Eyers, Nat. Chem. 6 (2014) 65–74, https://doi.org/10.1038/nchem.1817
[26] X.P. Li, L. Hang, T.T. Wang, Y.X. Leng, H. Zhang, Y.F. Meng, Z.B. Yin, W. Hang, J. Am. Chem. Soc. 143 (2021) 21648–21656, https://doi.org/10.1021/jacs.1c10081
[27] C.A. Patino, P. Mukherjee, E.J. Berns, E.H. Moully, L. Stan, M. Mrksich, H.D. Espinosa, ACS Nano 16 (2022) 7937–7946, https://doi.org/10.1021/acsnano.2c00698
[28] R. Frank, R. Hargreaves, Nat. Rev. Drug Discov. 2 (2003) 566–580, https://doi.org/10.1038/nrd1130
[29] D. Morel, D. Jeffery, S. Aspeslagh, G. Almouzni, S. Postel-Vinay, Nat. Rev. Clin. Oncol. 17 (2020) 91–107, https://doi.org/10.1038/s41571-019-0267-4
[30] F.N. Qu, F. Guilak, R.L. Mauck, Nat. Rev. Rheumatol. 15 (2019) 167–179, https://doi.org/10.1038/s41584-018-0151-0
[31] E. Infante, A. Castagnino, R. Ferrari, P. Monteiro, S. Agüera-González, P. Paul-Gilloteaux, M.J. Domingues, P. Maiuri, M. Raab, C.M. Shanahan, A. Baffet, M. Piel, E.R. Gomes, P. Chavrier, Nat. Commun. 9 (2018) 2443, https://doi.org/10.1038/s41467-018-04865-7
[32] P. Kaphle, Y.C. Li, L. Yao, J. Cell Physiol. 234 (2019) 3948–3960, https://doi.org/10.1002/jcp.27209
[33] A. Kumar, H.L. Ma, X. Zhang, K.Y. Huang, S.B. Jin, J. Liu, T. Wei, W.P. Cao, G.Z. Zou, X.-J. Liang, Biomaterials 33 (2012) 1180–1189, https://doi.org/10.1016/j.biomaterials.2011.10.058
[34] Z.L. Chai, D.N. Ran, L.W. Lu, C.Y. Zhan, H.T. Ruan, X.F. Hu, C. Xie, K. Jiang, J.Y. Li, J.F. Zhou, J. Wang, Y.Y. Zhang, R.H. Fang, L.F. Zhang, W.Y. Lu, ACS Nano 13 (2019) 5591–5601, https://doi.org/10.1021/acsnano.9b00661
[35] Y.Y. Fang, Y.T. Li, Y.Y. Li, R. He, Y. Zhang, X.B. Zhang, Y. Liu, H.X. Ju, Anal. Chem. 93 (2021) 7258–7265, https://doi.org/10.1021/acs.analchem.1c00469
[36] M. Yamamoto, H. Tsujishita, N. Hori, Y. Ohishi, S. Inoue, S. Ikeda, Y. Okada, J. Med. Chem. 41 (1998) 1209–1217, https://doi.org/10.1021/jm970404a
[37] B.V. Pipaliya, D.N. Trofimova, R.L. Grange, M. Aeluri, X. Deng, K. Shah, A.W. Craig, J.S. Allingham, P.A. Evans, J. Am. Chem. Soc. 143 (2021) 6847–6854, https://doi.org/10.1021/jacs.0c12404
[38] A. Rossello, E. Nuti, E. Orlandini, P. Carelli, S. Rapposelli, M. Macchia, F. Minutolo, L. Carbonaro, A. Albini, R. Benelli, G. Cercignani, G. Murphye, A. Balsamo, Bioorg. Med. Chem. 12 (2004) 2441–2450, https://doi.org/10.1016/j.bmc.2004.01.047
[39] Q. Li, S.H. Li, S.S. He, W. Chen, P.H. Cheng, Y. Zhang, Q.Q. Miao, K.Y. Pu, Angew. Chem. Int. Ed. 59 (2020) 7018–7023, https://doi.org/10.1002/anie.202000035
[40] W. Haiss, N.T.K. Thanh, J. Aveyard, D.G. Fernig, Anal. Chem. 79 (2007) 4215–4221, https://doi.org/10.1021/ac0702084
[41] Z.Y. Jiang, Y. Liu, R. Shi, X.R. Feng, W.G. Xu, X.L. Zhuang, J.X. Ding, X.S. Chen, Adv. Mater. 34 (2022) 2110094, https://doi.org/10.1002/adma.202110094
[42] C. Lv, Y. Lin, A.-A. Liu, Z.-Y. Hong, L. Wen, Z.F. Zhang, Z.-L. Zhang, H.Z. Wang, D.-W. Pang, Biomaterials 106 (2016) 69–77, https://doi.org/10.1016/j.biomaterials.2016.08.013
[43] X.Z. Ai, S.Y. Wang, Y.O. Duan, Q.Z. Zhang, M.S. Chen, W.W. Gao, L.F. Zhang, Biochemistry 60 (2021) 941–955, https://doi.org/10.1021/acs.biochem.0c00343
[44] J. Li, R.H. Lipson, Anal. Chem. 85 (2013) 6860–6865, https://doi.org/10.1021/ac401101j

[45] M. Boonrao, S. Yodkeeree, C. Ampasavate, S. Anuchapreeda, P. Limtrakul, Arch. Pharmacal Res 33 (2010) 989–998, https://doi.org/10.1007/s12272-010-0703-6
[46] Z. Lei, H. Zhang, Y.Q. Wang, X.Y. Meng, Z.X. Wang, Anal. Chem. 89 (2017) 6749–6757, https://doi.org/10.1021/acs.analchem.7b01037
[47] Y.P. Wang, T.T. Lin, W.Y. Zhang, Y.F. Jiang, H.Y. Jin, H.N. He, V.C. Yang, Y. Chen, Y.Z. Huang, Theranostics 5 (2015) 787–795, https://doi.org/10.7150/thno.11139
[48] M. Egeblad, Z. Werb, Nat. Rev. Cancer 2 (2002) 161–174, https://doi.org/10.1038/nrc745
[49] G. Giannelli, J. Falk-Marzillier, O. Schiraldi, W.G. Stetler-Stevenson, V. Quaranta, Science 277 (1997) 225–228, https://doi.org/10.1126/science.277.5323.225
[50] N. Koshikawa, G. Giannelli, V. Cirulli, K. Miyazaki, V. Quaranta, J. Cell Biol. 148 (2000) 615–624, https://doi.org/10.1083/jcb.148.3.615
[51] Q. Yu, I. Stamenkovic, Genes Dev. 13 (1999) 35–48, https://doi.org/10.1101/gad.13.1.35
[52] C. Bremer, C.-H. Tung, R. Weissleder, Nat. Med. 7 (2001) 743–748, https://doi.org/10.1038/89126
[53] G. Ferry, J.A. Boutin, P. Hennig, A. Genton, C. Desmet, J. Fauchere, G. Atassi, G.C. Tucker, Eur. J. Pharmacol. 351 (1998) 225–233, https://doi.org/10.1016/S0014-2999(98)00304-5

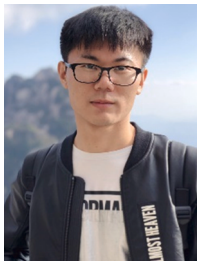

Nan Feng received his B.S. degree from Nanjing University. He is a Ph.D. candidate in Prof. Huangxian Ju's group at Nanjing University. His research focuses on mass spectrometric biosensing and imaging.

Yiran Li received his master's degree in chemistry from Northwest Normal University. He is a Ph.D. candidate in Prof. Huangxian Ju's group at Nanjing University. His supervisor is Prof. Lin Ding. His research focuses on disease-related glycan analysis and manipulation of biological functions through glycan editing.

Jiahui Sun is pursuing her Ph.D. in analytical chemistry at Nanjing University. Her research interests include multiplex detection and imaging of biomarkers using functional mass nanoprobes.

Haiqi Wang received his B.S. degree in School of Chemistry and Chemical Engineering from Nanjing University in 2020. Since then, he has studied as a Ph.D. candidate in Prof. Huangxian Ju's group at Nanjing University. His research focuses on glycans and glycan-related processes.

Qiulin Ma received her bachelor's degree in chemistry from Beijing Normal University in 2017 and her master's degree in chemistry from Nanjing University in 2020. She is currently pursuing her Ph.D. in the field of chemical biology at McMaster University, where her research is focusing on utilizing nuclear magnetic resonance to investigate the structural basis of heparin-induced thrombocytopenia associated with platelet factor 4 (PF4). Her work aims to elucidate the complex interactions between PF4, polyanions and antibodies.

Dr. Jingxing Guo received his B.S. degree from Wuhan University in 2014 and Ph.D. degree from Nanjing University in 2019. Then he was a postdoctoral fellow in Jinling Hospital from 2019 to 2022. Now he is an associate professor in Wuhan University of Technology. His research focuses on combing Raman spectroscopy with artificial intelligence for probing structures and functions of proteins, as well as point-of-care testing of disease markers in clinical samples.

Huangxian Ju received his BS, MS and Ph.D. degrees from Nanjing University during 1982–1992. He was a postdoc at Montreal University (Canada) during 1996–1997 and a guest professor at three universities in Germany and Ireland from 1999 to 2000. He is currently the director of the State Key Laboratory of Analytical Chemistry for Life Science, a Chief Scientist of the National Key Basic Research Program ('973 Program'), an Awardee of the National Science Fund for Distinguished Young Scholars, Chang Jiang Scholars Program and the 2022 Advances in Measurement Science Lectureship Award. His research focus on nanobiosensing, analytical biochemistry and molecular diagnosis. He has published 858 papers in different journals with h-index of 103 (Google Scholar h-index 113 with more than 48000 citations).